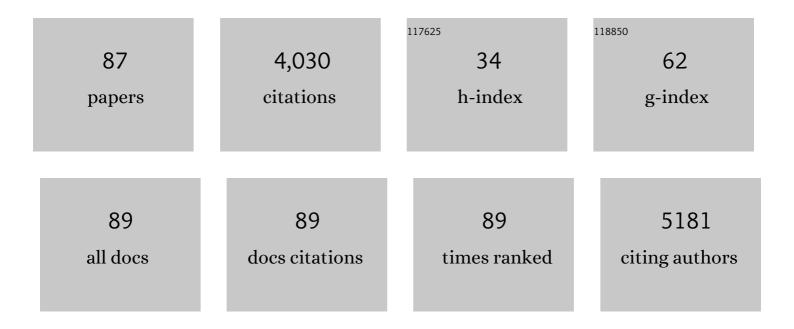
List of Publications by Year in descending order

Source: https://exaly.com/author-pdf/8545748/publications.pdf Version: 2024-02-01



LING FENG

#	Article	IF	CITATIONS
1	Ligand-Induced Nucleation Growth Kinetics of CdTe QDs: Implications for White-Light-Emitting Diodes. ACS Applied Nano Materials, 2022, 5, 401-410.	5.0	3
2	Ultra-small bimetallic phosphides for dual-modal MRI imaging guided photothermal ablation of tumors. Dalton Transactions, 2022, 51, 4423-4428.	3.3	7
3	Double perovskite Cs ₂ NaInCl ₆ nanocrystals with intense dual-emission <i>via</i> self-trapped exciton-to-Tb ³⁺ dopant energy transfer. Journal of Materials Chemistry C, 2022, 10, 10609-10615.	5.5	32
4	Nanocomposites based on lanthanide-doped upconversion nanoparticles: diverse designs and applications. Light: Science and Applications, 2022, 11, .	16.6	58
5	Remarkably Enhanced Red Upconversion Emission in β-NaLuF ₄ :Er,Tm Microcrystals via Ion Exchange. Inorganic Chemistry, 2022, 61, 10713-10721.	4.0	8
6	Recent Advances in Graphitic Carbon Nitride Supported Singleâ€Atom Catalysts for Energy Conversion. ChemCatChem, 2021, 13, 1250-1270.	3.7	46
7	Tunable ultra-uniform Cs ₄ PbBr ₆ perovskites with efficient photoluminescence and excellent stability for high-performance white light-emitting diodes. Journal of Materials Chemistry C, 2021, 9, 12811-12818.	5.5	4
8	Investigation on the photoluminescence and thermoluminescence of BaGa ₂ O ₄ :Bi ³⁺ at extremely low temperatures. Journal of Materials Chemistry C, 2021, 9, 1786-1793.	5.5	18
9	Engineering Cu _{2â^'<i>x</i>} S-conjugated upconverting nanocomposites for NIR-II light-induced enhanced chemodynamic/photothermal therapy of cancer. Journal of Materials Chemistry B, 2021, 9, 7216-7228.	5.8	9
10	Proteinaceous Fibers with Outstanding Mechanical Properties Manipulated by Supramolecular Interactions. CCS Chemistry, 2021, 3, 1669-1677.	7.8	39
11	Near-Infrared-Light-Responsive Copper Oxide Nanoparticles as Efficient Theranostic Nanoagents for Photothermal Tumor Ablation. ACS Applied Bio Materials, 2021, 4, 5266-5275.	4.6	12
12	In Situ Embedding Synthesis of Highly Stable CsPbBr ₃ /CsPb ₂ Br ₅ @PbBr(OH) Nano/Microspheres through Water Assisted Strategy. Advanced Functional Materials, 2021, 31, 2103275.	14.9	42
13	Embellishment of Upconversion Nanoparticles with Ultrasmall Perovskite Quantum Dots for Fullâ€Color Tunable, Dualâ€Modal Luminescence Anticounterfeiting. Advanced Optical Materials, 2021, 9, 2100814.	7.3	31
14	One-step conversion of CsPbBr ₃ into Cs ₄ PbBr ₆ /CsPbBr ₃ @Ta ₂ O ₅ core–shell microcrystals with enhanced stability and photoluminescence. Journal of Materials Chemistry C, 2021, 9, 1228-1234.	5.5	14
15	Selenium Vacancy Engineering Using Bi ₂ Se ₃ Nanodots for Boosting Highly Efficient Photonic Hyperthermia. ACS Applied Materials & Interfaces, 2021, 13, 48378-48385.	8.0	5
16	Simultaneous Enhancement of Photoluminescence and Stability of CsPbCl ₃ Perovskite Enabled by Titanium Ion Dopant. Journal of Physical Chemistry Letters, 2021, 12, 10746-10752.	4.6	12
17	Investigation of 4 <i>f</i> â€Related Electronic Transitions of Rareâ€Earth Doped ZnO Luminescent Materials: Insights from Firstâ€Principles Calculations. ChemPhysChem, 2020, 21, 51-58.	2.1	23
18	Decoration of upconversion nanocrystals with metal sulfide quantum dots by a universal <i>in situ</i> controlled growth strategy. Nanoscale, 2020, 12, 3977-3987.	5.6	13

#	Article	IF	CITATIONS
19	Design of a mixed-anionic-ligand system for a blue-light-excited orange-yellow emission phosphor Ba _{1.31} Sr _{3.69} (BO ₃) ₃ Cl:Eu ²⁺ . Journal of Materials Chemistry C, 2020, 8, 3040-3050.	5.5	31
20	Unveiling the Relationship between Energy Transfer and the Triplet Energy Level by Tuning Diarylethene within Europium(III) Complexes. Inorganic Chemistry, 2020, 59, 661-668.	4.0	9
21	Insight into the Characteristics of 4f-Related Electronic Transitions for Rare-Earth-Doped KLuS ₂ Luminescent Materials through First-Principles Calculation. Journal of Physical Chemistry C, 2020, 124, 932-938.	3.1	8
22	In situ decorating of ultrasmall Ag2Se on upconversion nanoparticles as novel nanotheranostic agent for multimodal imaging-guided cancer photothermal therapy. Applied Materials Today, 2020, 18, 100497.	4.3	26
23	Unveiling the mechanism of rare earth doping to optimize the optical performance of the CsPbBr ₃ perovskite. Inorganic Chemistry Frontiers, 2020, 7, 4669-4676.	6.0	15
24	Engineering Gadoliniumâ€Integrated Tellurium Nanorods for Theoryâ€Oriented Photonic Hyperthermia in the NIRâ€II Biowindow. Small, 2020, 16, 2003508.	10.0	7
25	Emerging biomaterials: Taking full advantage of the intrinsic properties of rare earth elements. Nano Today, 2020, 35, 100952.	11.9	32
26	Study of a color-tunable long afterglow phosphor Gd _{1.5} Y _{1.5} Ga ₃ Al ₂ O ₁₂ :Tb ³⁺ : luminescence properties and mechanism. RSC Advances, 2020, 10, 28049-28058.	3.6	15
27	Lanthanide-doped bismuth-based fluoride nanoparticles: controlled synthesis and ratiometric temperature sensing. CrystEngComm, 2020, 22, 3432-3438.	2.6	10
28	In Situ Construction of Pt–Ni NF@Niâ€MOFâ€74 for Selective Hydrogenation of <i>p</i> â€Nitrostyrene by Ammonia Borane. Chemistry - A European Journal, 2020, 26, 12539-12543.	3.3	9
29	Selective enhancement of green upconversion luminescence from NaYF4:Yb, Er microparticles through Ga3+ doping for sensitive temperature sensing. Journal of Luminescence, 2019, 215, 116632.	3.1	26
30	Renal Clearable Bi–Bi ₂ S ₃ Heterostructure Nanoparticles for Targeting Cancer Theranostics. ACS Applied Materials & Interfaces, 2019, 11, 7774-7781.	8.0	38
31	A highly active (102) surface-induced rapid degradation of a CuS nanotheranostic platform for <i>in situ T</i> ₁ -weighted magnetic resonance imaging-guided synergistic therapy. Nanoscale, 2019, 11, 12853-12857.	5.6	33
32	Commendable Pr ³⁺ -activated Ba ₂ Ga ₂ GeO ₇ phosphor with high-brightness white long-persistent luminescence. Journal of Materials Chemistry C, 2019, 7, 6698-6705.	5.5	44
33	A strategy for developing thermal-quenching-resistant emission and super-long persistent luminescence in BaGa ₂ O ₄ :Bi ³⁺ . Journal of Materials Chemistry C, 2019, 7, 13088-13096.	5.5	42
34	Enhanced upconversion luminescence and controllable phase/shape of NaYF ₄ :Yb/Er crystals through Cu ²⁺ ion doping. CrystEngComm, 2018, 20, 1945-1953.	2.6	59
35	A new blue long-lasting phosphorescence phosphor Mg2SnO4:Bi3+: synthesis and luminescence properties. Journal of Materials Science: Materials in Electronics, 2018, 29, 4163-4170.	2.2	10
36	Near-infrared optical and X-ray computed tomography dual-modal imaging probe based on novel lanthanide-doped K _{0.3} Bi _{0.7} F _{2.4} upconversion nanoparticles. Nanoscale, 2018, 10, 1394-1402.	5.6	45

#	Article	IF	CITATIONS
37	Multifunctional Cu–Ag ₂ S nanoparticles with high photothermal conversion efficiency for photoacoustic imaging-guided photothermal therapy <i>in vivo</i> . Nanoscale, 2018, 10, 825-831.	5.6	68
38	Origin of Color Centers in the Perovskite Oxide CeAlO ₃ . ChemPlusChem, 2018, 83, 976-983.	2.8	8
39	Thermal Decomposition of CdS Nanowires Assisted by ZIF-67 to Induce the Formation of Co ₉ S ₈ -Based Carbon Nanomaterials with High Lithium-Storage Abilities. ACS Applied Energy Materials, 2018, 1, 6242-6249.	5.1	8
40	Synthesis and Luminescence Properties of Bi ³⁺ -Activated K ₂ MgGeO ₄ : A Promising High-Brightness Orange-Emitting Phosphor for WLEDs Conversion. Inorganic Chemistry, 2018, 57, 12303-12311.	4.0	142
41	Simple construction of Cu _{2â^x} S:Pt nanoparticles as nanotheranostic agent for imaging-guided chemo-photothermal synergistic therapy of cancer. Nanoscale, 2018, 10, 10945-10951.	5.6	23
42	Developing near-infrared long-lasting phosphorescence of Yb ³⁺ through a medium: insights into energy transfer in the novel material Zn _{1.98} Li _{0.02} P ₂ O ₇ :Yb ³⁺ . Dalton Transactions, 2018, 47, 9814-9823.	3.3	9
43	Ultrafast synthesis of ultrasmall polyethylenimine-protected AgBiS ₂ nanodots by "rookie method―for <i>in vivo</i> dual-modal CT/PA imaging and simultaneous photothermal therapy. Nanoscale, 2018, 10, 16765-16774.	5.6	44
44	Self-supported Co3O4wire-penetrated-cage hybrid arrays with enhanced supercapacitance properties. CrystEngComm, 2017, 19, 1459-1463.	2.6	11
45	A Simple Strategy for the Controlled Synthesis of Ultrasmall Hexagonalâ€Phase NaYF ₄ :Yb,Er Upconversion Nanocrystals. ChemPhotoChem, 2017, 1, 369-375.	3.0	18
46	PEGylated GdF ₃ :Fe Nanoparticles as Multimodal <i>T</i> ₁ / <i>T</i> ₂ -Weighted MRI and X-ray CT Imaging Contrast Agents. ACS Applied Materials & Interfaces, 2017, 9, 20426-20434.	8.0	45
47	The size-responsive phase transition mechanism and upconversion/downshifting luminescence properties of KLu ₂ F ₇ :Yb ³⁺ /Er ³⁺ nanocrystals. Journal of Materials Chemistry C, 2017, 5, 6311-6318.	5.5	8
48	Ultrafast Synthesis of Novel Hexagonal Phase NaBiF ₄ Upconversion Nanoparticles at Room Temperature. Advanced Materials, 2017, 29, 1700505.	21.0	131
49	Achieving the Tradeâ€Off between Selectivity and Activity in Semihydrogenation of Alkynes by Fabrication of (Asymmetrical Pd@Ag Core)@(CeO ₂ Shell) Nanocatalysts via Autoredox Reaction. Advanced Materials, 2017, 29, 1605332.	21.0	73
50	A pH-responsive assembly based on upconversion nanocrystals and ultrasmall nickel nanoparticles. Journal of Materials Chemistry C, 2017, 5, 9666-9672.	5.5	10
51	Benefits of surfactant effects on quantum efficiency enhancement and temperature sensing behavior of NaBiF ₄ upconversion nanoparticles. Journal of Materials Chemistry C, 2017, 5, 9659-9665.	5.5	60
52	Ultrafast Synthesis of Ultrasmall Poly(Vinylpyrrolidone)â€Protected Bismuth Nanodots as a Multifunctional Theranostic Agent for In Vivo Dualâ€Modal CT/Photothermalâ€Imagingâ€Guided Photothermal Therapy. Advanced Functional Materials, 2017, 27, 1702018.	14.9	203
53	A Metal–Organic Framework/DNA Hybrid System as a Novel Fluorescent Biosensor for Mercury(II) Ion Detection. Chemistry - A European Journal, 2016, 22, 477-480.	3.3	155
54	Zn or O? An Atomic Level Comparison on Antibacterial Activities of Zinc Oxides. Chemistry - A European Journal, 2016, 22, 8053-8058.	3.3	30

#	Article	IF	CITATIONS
55	Optimization of Bi ³⁺ in Upconversion Nanoparticles Induced Simultaneous Enhancement of Near-Infrared Optical and X-ray Computed Tomography Imaging Capability. ACS Applied Materials & amp; Interfaces, 2016, 8, 27490-27497.	8.0	72
56	A "Solid Dualâ€ionsâ€Transformation―Route to S,N Coâ€Doped Carbon Nanotubes as Highly Efficient "Metalâ€Free―Catalysts for Organic Reactions. Advanced Materials, 2016, 28, 10679-10683.	21.0	107
57	Core–shell–shell heterostructures of α-NaLuF ₄ :Yb/Er@NaLuF ₄ :Yb@MF ₂ (M = Ca, Sr, Ba) with remarkably enhanced upconversion luminescence. Dalton Transactions, 2016, 45, 11129-11136.	3.3	15
58	Dual-functional α-NaYb(Mn)F4:Er3+@NaLuF4 nanocrystals with highly enhanced red upconversion luminescence. RSC Advances, 2016, 6, 33493-33500.	3.6	5
59	An ideal detector composed of a 3D Gd-based coordination polymer for DNA and Hg ²⁺ ion. Inorganic Chemistry Frontiers, 2016, 3, 376-380.	6.0	37
60	Lanthanide doped Bi ₂ O ₃ upconversion luminescence nanospheres for temperature sensing and optical imaging. Dalton Transactions, 2016, 45, 2686-2693.	3.3	67
61	Core–shell BaYbF ₅ :Tm@BaGdF ₅ :Yb,Tm nanocrystals for in vivo trimodal UCL/CT/MR imaging. RSC Advances, 2016, 6, 14283-14289.	3.6	21
62	CeO ₂ nanowires self-inserted into porous Co ₃ O ₄ frameworks as high-performance "noble metal free―hetero-catalysts. Chemical Science, 2016, 7, 1109-1114.	7.4	74
63	Encapsulation of Ln ^{III} Ions/Dyes within a Microporous Anionic MOF by Postâ€synthetic Ionic Exchange Serving as a Ln ^{III} Ion Probe and Twoâ€Color Luminescent Sensors. Chemistry - A European Journal, 2015, 21, 9748-9752.	3.3	123
64	Strongly Coupled Pt–Ni ₂ GeO ₄ Hybrid Nanostructures as Potential Nanocatalysts for CO Oxidation. Chemistry - A European Journal, 2015, 21, 14768-14771.	3.3	5
65	Yb ³⁺ /Er ³⁺ -Codoped Bi ₂ O ₃ Nanospheres: Probe for Upconversion Luminescence Imaging and Binary Contrast Agent for Computed Tomography Imaging. ACS Applied Materials & Interfaces, 2015, 7, 26346-26354.	8.0	78
66	Visibleâ€nearâ€infrared luminescent lanthanide ternary complexes based on betaâ€diketonate using visibleâ€light excitation. Luminescence, 2015, 30, 1071-1076.	2.9	22
67	Growth of lanthanide-doped LiGdF4 nanoparticles induced by LiLuF4 core as tri-modal imaging bioprobes. Biomaterials, 2015, 65, 115-123.	11.4	55
68	Microwave-assisted synthesis of nanoscale Eu(BTC)(H2O)·DMF with tunable luminescence. Science China Chemistry, 2015, 58, 973-978.	8.2	13
69	Nd ³⁺ -sensitized NaLuF ₄ luminescent nanoparticles for multimodal imaging and temperature sensing under 808 nm excitation. Nanoscale, 2015, 7, 17861-17870.	5.6	74
70	α-NaYb(Mn)F ₄ :Er ³⁺ /Tm ³⁺ @NaYF ₄ UCNPs as "Band-Shape―Luminescent Nanothermometers over a Wide Temperature Range. ACS Applied Materials & Interfaces, 2015, 7, 20813-20819.	8.0	114
71	A long-wave optical pH sensor based on red upconversion luminescence of NaGdF ₄ nanotubes. RSC Advances, 2014, 4, 55897-55899.	3.6	16
72	Visible and near-infrared luminescent mesoporous titania microspheres functionalized with lanthanide complexes: microstructure and luminescence with visible excitation. RSC Advances, 2014, 4, 28481.	3.6	26

#	Article	IF	CITATIONS
73	Pure and intense orange upconversion luminescence of Eu3+ from the sensitization of Yb3+–Mn2+ dimer in NaY(Lu)F4 nanocrystals. Journal of Materials Chemistry C, 2014, 2, 9004-9011.	5.5	38
74	Rare earth fluorides upconversion nanophosphors: from synthesis to applications in bioimaging. CrystEngComm, 2013, 15, 7142.	2.6	54
75	Microwave-assisted synthesis and down- and up-conversion luminescent properties of BaYF5:Ln (Ln =) Tj ETQq1 1	1 0.784314 2.6	1 rgBT /Over
76	Hybrid materials based on lanthanide organic complexes: a review. Chemical Society Reviews, 2013, 42, 387-410.	38.1	674
77	Phase-tunable synthesis and upconversion photoluminescence of rare-earth-doped sodium scandium fluoride nanocrystals. CrystEngComm, 2013, 15, 6901.	2.6	22
78	Facile and rapid fabrication of nanostructured lanthanide coordination polymers as selective luminescent probes in aqueous solution. Journal of Materials Chemistry, 2012, 22, 6819.	6.7	161
79	High-Brightness, Broad-Spectrum White Organic Electroluminescent Device Obtained by Designing Light-Emitting Layers as also Carrier Transport Layers. Journal of Physical Chemistry C, 2010, 114, 21723-21727.	3.1	17
80	Novel Multifunctional Nanocomposites: Magnetic Mesoporous Silica Nanospheres Covalently Bonded with Near-Infrared Luminescent Lanthanide Complexes. Langmuir, 2010, 26, 3596-3600.	3.5	78
81	Fabrication and characterization of magnetic mesoporous silica nanospheres covalently bonded with europium complex. Dalton Transactions, 2010, 39, 5166.	3.3	15
82	A study on the near-infrared luminescent properties of xerogel materials doped with dysprosium complexes. Dalton Transactions, 2009, , 6593.	3.3	53
83	Near-infrared luminescent xerogel materials covalently bonded with ternary lanthanide [Er(iii), Nd(iii), Yb(iii), Sm(iii)] complexes. Dalton Transactions, 2009, , 2406.	3.3	57
84	Erbiumâ€Complexâ€Doped Nearâ€Infrared Luminescent and Magnetic Macroporous Materials. European Journal of Inorganic Chemistry, 2008, 2008, 5513-5518.	2.0	12
85	Hydrothermal synthesis and crystal structure of a new two-dimensional zinc citrate complex. Journal of Coordination Chemistry, 2005, 58, 1581-1588.	2.2	30
86	STRUCTURAL PHASE TRANSITION IN THE LAYERED PEROVSKITE COMPOUND BaTb2Mn2O7., 2002, , .		0
87	X-RAY ABSORPTION STUDY OF ELECTRONIC, SPATIAL STRUCTURE AND PROPERTIES OF BaLn2Mn2O7 MANGANATES. , 2002, , .		0